Out-of-equilibrium microrheology inside living cells

Claire Wilhelm

▶ **To cite this version:**

Claire Wilhelm. Out-of-equilibrium microrheology inside living cells. Physical Review Letters, 2008, 101 (2), pp.028101. 10.1103/PhysRevLett.101.028101 . hal-00315471

HAL Id: hal-00315471
https://hal.science/hal-00315471

Submitted on 5 Jun 2023

HAL is a multi-disciplinary open access archive for the deposit and dissemination of scientific research documents, whether they are published or not. The documents may come from teaching and research institutions in France or abroad, or from public or private research centers.

L'archive ouverte pluridisciplinaire **HAL**, est destinée au dépôt et à la diffusion de documents scientifiques de niveau recherche, publiés ou non, émanant des établissements d'enseignement et de recherche français ou étrangers, des laboratoires publics ou privés.

Distributed under a Creative Commons Attribution 4.0 International License

Out-of-Equilibrium Microrheology inside Living Cells

Claire Wilhelm*

Laboratoire Matière et Systèmes Complexes (MSC), UMR 7057, CNRS and University Paris Diderot, Paris, France

(Received 12 December 2007; published 9 July 2008)

Both forced and spontaneous motions of magnetic microbeads engulfed by *Dictyostelium* cells have served as experimental probes of intracellular dynamics. The complex shear modulus $G^*(\omega)$, determined from active oscillatory measurements, has a power-law dynamics and increases with the probe size, reflecting intracellular structural complexity. The combined use of passive microrheology allows one to derive the power spectrum of active forces acting on intracellular phagosomes and to test the validity of the fluctuation-dissipation theorem inside living cells.

DOI: 10.1103/PhysRevLett.101.028101 PACS numbers: 87.17.Rt, 83.85.Cg, 87.16.Uv, 87.80.Fe

During the diverse processes that govern the survival and development of living organisms, each cell must react continuously, in a perfectly orchestrated manner, to a variety of internal and external constraints. During the past two decades, micromanipulations have been developed to mechanically deform living cells in a controlled manner. Most of these approaches target the whole cell [1] or involve local constraints applied to the cell surface [2–4]. Biophysical methods capable of deforming the intracellular environment (active intracellular microrheology) are rare, however, because of the experimental difficulties inherent in introducing a probe into a living cell and manipulating it in a ''noninvasive'' manner. Some recent reports describe the use of engulfed magnetic microbeads or endocytosed magnetic nanoparticles submitted to a magnetic force [5] or torque [6] and embedded granules submitted to optical forces [7]. However, most studies of intracellular mechanics have focused on spontaneous displacement of intracellular granules or internalized microbeads in order to deduce local dynamic properties (passive intracellular microrheology) [8–10].

In an in-equilibrium system, the fluctuation-dissipation theorem (FDT) links thermal fluctuations (passive measurements) to the response to external perturbation (active measurements). For biological systems, recent studies have shown the violation of the FDT. Deviation from equilibrium has been observed with an *in vitro* model system consisting of an actin network with embedded myosin motors [11] and has been pioneered for living cells by Bursac *et al.* [12]. In this case, violation of the FDT was reported by comparing both forced and spontaneous motions of magnetic beads attached to the cell membrane and bound to deeper structures of the cytoskeleton. Inside the cell, in the cytoplasm, direct evidence of the deviation from equilibrium is lacking. In this Letter, the combination of active and passive intracellular microrheology is used to explore internal cell mechanics, with respect to probe size and to the activity of intracellular motors.

Magnetic beads of various sizes (0.3–1–2.8 μm diameter) were engulfed inside the cytoplasm of *Dictyostelium* cells by the process of phagocytosis. When submitted to an external magnetic field, these so-obtained ''magnetic phagosomes'' acquire a magnetic moment m and self-organize in chains containing N beads, as shown in Figs. 1 (electron microscopy) and 2(a) (videomicroscopy).

The active microrheology experiments were based on the recently developed rotational magnetic microrheology approach [13], in which chains of magnetic microbeads are manipulated by means of a sinusoidally oscillating magnetic field [Fig. 2(b)]. Briefly, the magnetic torque applied to a chains of N beads $\Gamma_m = \Gamma_o^* \sin[2(\beta - \theta)]/2$ balances the viscoelastic torque $\Gamma_{ve} = \kappa V G \theta$. The magnetic and geometric factors Γ_o and κ are given in Ref. [13]. G is the material intrinsic complex shear modulus $G^*(\omega) = G'(\omega) + iG''(\omega)$, where G' and G'' relate to the elastic and viscous responses, respectively. Angles $\beta = \beta_o e^{i\omega t}$ and $\theta = \theta_o e^{i\omega t - i\phi}$ are described in Fig. 2(b). For small $(\beta - \theta)$ values, $\Gamma_m = \Gamma_{ve}$ gives G' and G'' as a function of the loss of amplitude θ_o/β_o and the phase lag ϕ of the chains: $G' = (\Gamma_o/\kappa V)\{(\beta_o/\theta_o)^* \sin(\phi) - 1\}$ and $G'' = (\Gamma_o/\kappa V)^*(\beta_o/\theta_o)^* \sin(\phi)$. Videomicroscopy with an ultrafast camera (up to 1000 frames per second) was used to detect the chain oscillations at frequencies varying from 0.2 to 20 Hz. The oscillation of at least 20 different chains, in different cells, was analyzed for a given number N of

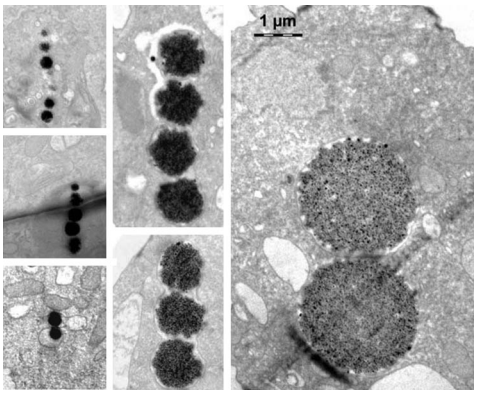

FIG. 1. Electron micrographs of the *Dictyostelium* cell interior containing chains of magnetic beads within phagosomes arranged along the magnetic field direction.

 © 2008 The American Physical Society

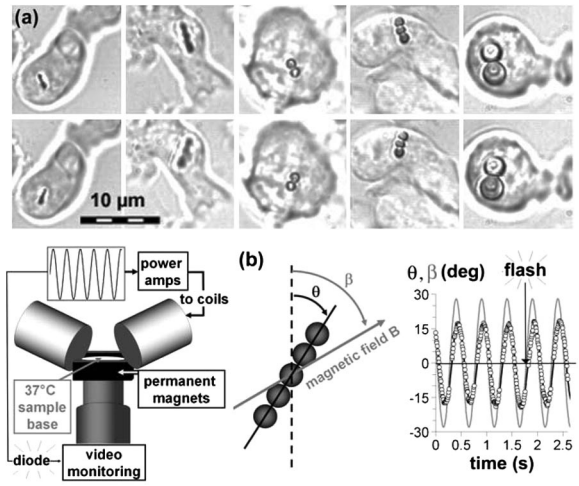

FIG. 2. (a) Oscillation of chains of magnetic phagosomes (1 Hz − $\beta_o = 28°$) containing (from left to right) 0.3-, 1-, and 2.8-μm-diameter magnetic beads, studied by means of video-microscopy. Videos are available in supplementary auxiliary files [18]. (b) The magnetic device used for microrheological measurements inside the cell (left): Two permanent magnets create a homogeneous field of 79 mT, and a perpendicular pair of coils is supplied with the same current intensity (2 and 4 A), providing a magnetic field of 21 and 42 mT, respectively. Angle notations (middle) and typical angular response curve (right).

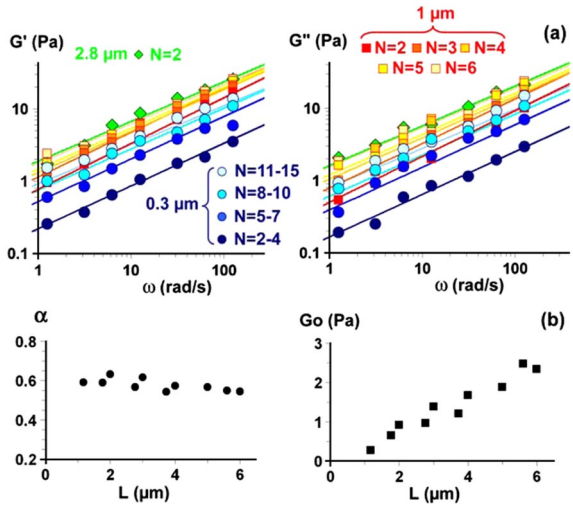

FIG. 3 (color online). (a) Mean values of $G'(\omega)$ and $G''(\omega)$ obtained with different probe sizes. Deviation (not shown for clarity) was in the range of 40% for every measure. The solid lines are the fit of Eq. (1) $G^*(\omega) = G_o(i\omega/\omega_o)^\alpha$ to the data. For chains containing two beads ($N = 2$), $G_o = (0.27 \pm 0.04)$ Pa, $G_o = (0.92 \pm 0.06)$ Pa, and $G_o = (2.47 \pm 0.1)$ Pa and $\alpha = (0.59 \pm 0.03)$, $\alpha = (0.63 \pm 0.02)$, and $\alpha = (0.55 \pm 0.03)$ for beads of 0.3, 1, and 2.8 μm diameters, respectively. (b) Exponent α and prefactor G_o as a function of the probe length $L = Nd$, with N the number of beads in the chain probe and d the bead diameter.

beads in the chain, at a given frequency, and for two different angles β_o (15.5° and 28°). No deviation was observed for different β_o values, ensuring the linearity of the measurement. Both G' and G'' increased with frequency [Fig. 3(a)] and followed a power law ω^α, with the same exponent α of between 0.5 and 0.6. The G'/G'' ratio did not vary with frequency and was found close to 1, and all of the data could be fitted [Fig. 3(a)] with a power-law constant phase model for the complex shear modulus:

$$G^*(\omega) = G_o(i\omega/\omega_o)^\alpha, \quad (1)$$

with $\omega_o = 1\ \mathrm{s}^{-1}$. Values for G_o and α are given in the Fig. 3 caption.

This power-law behavior is inconsistent with the discrete number of time constants predicted by simple viscoelastic models [5,14]. The power-law exponent α is indicative of the degree of solid- or liquidlike mechanical behavior of the probed material (solidlike for $\alpha = 0$ and fluidlike for $\alpha = 1$). The exponent found here for the intracellular rheological behavior ($\alpha = 0.5$–0.6) is much larger than that obtained when a cell is stretched between microplates ($\alpha = 0.2$–0.3) [1], locally deformed by torque ($\alpha = 0.2$–0.25) [2] or force ($\alpha = 0.18$–0.21) [4] exerted on membrane-bound microbeads or poked with a microtip ($\alpha = 0.22$) [3]. This is in keeping with the only other active microrheology study inside the cell which yielded power-law behavior with an exponent of 0.5 by measuring the response of intracellular granules trapped and displaced with optical tweezers [7]. Results of intracellular passive one-point microrheology experiments measuring fluctuations of intracellular particles or granule positions submitted only to thermal forces also yielded an exponent of 0.5 [8]. Interestingly, the exponent was 0.33 in lamellar regions, which more closely resemble the cortical cytoskeleton. Our active measurements therefore support an intracellular medium that is much more fluidlike than the membrane and cortical cytoskeleton, with almost equivalent elastic and dissipative contributions.

The major finding concerns the dependence of the rheological measurement with the probe size: Figure 3(b) shows changes in the exponent α and the prefactor G_o as a function of the length of the probed chains. Although α varies very little with the probe size, G_o increases linearly, by 1 order of magnitude (from 0.27 to 2.4 Pa), when the chain length L increases from hundreds of nanometers to the scale of the whole cell. This increase reflects a stiffer medium at larger scales, coherent with structural complexity and the involvement of more elements probed while increasing the probe size. Indeed, among thousands of components contributing to the architecture of the cytoplasm, intracellular membranes have a length ranging from nanometers to a few microns, and intracellular cytoskeleton filaments organize into fibers a few microns long or remain isolated with a typical length of a few nanometers.

The disposal of an active magnetic probe microrheological measurement and its comparison with spontaneous motion of embedded probes opens a new window to explore the deviation from equilibrium inside living cells and to evaluate the forces generated by molecular motors. The

spontaneous motion of a single phagosome within the cytoplasm is described by a generalized Langevin equation $m\frac{dv}{dt} + \int_0^t \zeta(t-\tau)v(\tau)d\tau = F(t)$, in which $v(t)$ is the phagosome velocity, $\zeta(t)$ a delayed friction function that takes into account the viscoelastic properties, and $F(t)$ the force acting on the phagosome, including contributions of both thermal Brownian forces and driving forces generated by molecular motors.

Assuming that inertia is negligible for micron-sized phagosomes of diameter a and that generalization of Stokes law to viscoelastic materials states that $G(\omega) = \frac{(i\omega)\zeta(\omega)}{6\pi a}$, the Fourier transforms of $F(t)$ and $v(t)$ are linked as $F(\omega) = \frac{6\pi a G(\omega)}{(i\omega)} v(\omega)$. The power spectrum of intracellular forces $P_{FF}(\omega)$, a Fourier transform of the correlation function $\langle F(t)F(t+\tau)\rangle_t$, then writes $P_{FF}(\omega) = \frac{|6\pi a G^*(\omega)|^2}{\omega^2} P_{vv}(\omega)$, with $P_{vv}(\omega)$ related to Fourier transform $\langle r^2(\omega)\rangle$ of the mean square displacement (MSD) $\langle r^2(t)\rangle$: $\omega^2\langle r^2(\omega)\rangle = 4P_{vv}(\omega)$. $P_{FF}(\omega)$ can therefore be calculated from the correlation function and shear modulus as

$$P_{FF}(\omega) = (3\pi a)^2 |G^*(\omega)|^2 \langle r^2(\omega)\rangle. \quad (2)$$

In the absence of driving forces (at thermal equilibrium), the FDT writes

$$\langle r^2(\omega)\rangle = 4k_B T \frac{\alpha''(\omega)}{\omega}, \quad (3)$$

where $\alpha^*(\omega) = \alpha'(\omega) - \alpha''(\omega) = \frac{1}{6\pi a G^*(\omega)}$, giving

$$P_{FF}(\omega) = (6\pi a) k_B T \frac{G''(\omega)}{\omega}. \quad (4)$$

The fluctuation-dissipation theorem [Eqs. (3) and (4)] is no longer valid for systems out of equilibrium, as it is presumed for living cells, owing, in particular, to the activity of molecular motors. Evaluation of $P_{FF}(\omega)$ for intracellular forces was first proposed in Ref. [10], where it was demonstrated that the sub- versus superdiffusive behaviors of intracellular granules versus phagosomes can be related to the activity of associated microtubule motors. More recently, Lau *et al.* [15] calculated the power spectrum of stress fluctuations by comparing passive measurements made with intracellular granules to active measurements described by Fabry *et al.* [2] using magnetic beads coupled through the membrane to the cortical cytoskeleton. However, both measurements are indirect, as the active and passive probes differ, with different cellular locations, hindering the quantification of motor activities. Here correlation [passive microrheology, $\langle r^2(\omega)\rangle$] and response functions [active microrheology, $G^*(\omega)$] were obtained independently with the same probes, with the same intracellular location. For the passive microrheology measurements, the magnetic phagosomes 0.3, 1.0, and 2.8 μm in diameter were tracked every 0.01 s and the mean square displacement $\langle r^2(t)\rangle$ computed [see Fig. 4(a)]. The MSDs of all beads were well described by power-law behavior over the range $0.01 < t < 4$ s: $\langle r^2(t)\rangle = D^*(t/t_o)^\beta$, with β between 1.2 and 1.6 for all three types of beads, demonstrating superdiffusive behavior. t_o is taken to be 1 s, and D^* is expressed in units of m^2. For each MSD, the power spectral density was computed by Fourier transform, and its mean value could be adjusted by a single power law [Fig. 4(a)]

$$\langle r^2(\omega)\rangle = D\left(\frac{\omega}{\omega_o}\right)^{-(\beta+1)}. \quad (5)$$

ω_o is taken to be 1 s^{-1}, and D is expressed in units of m^2 s. Values for D and β are given in the Fig. 4 caption. For the active microrheology measurements, $G^*(\omega)$ is taken as the measure made in the same cells with the same probes, using doublets of beads ($N = 2$), to approach the one-bead probe conditions used for fluctuations. $P_{FF}(\omega)$ then follows a power-law behavior $P_{FF}(\omega) \sim \omega^{-\lambda}$, with $\lambda = \beta + 1 - 2\alpha$. With thermal equilibrium, $\lambda = 1 - \alpha$. Violation of this relationship was first observed with a probe strongly coupled to an actin cytoskeleton via the cell membrane, placing λ around 2 [12], as first suggested by Lau *et al.* [15]. Here, with the use of intracellular probes, λ was found around 1.2. The value $\lambda = 2$ corresponds to a series of force steps, while $\lambda = 0$ corresponds to a series of instantaneous infinite force pulses (uncorrelated spectrum). A value in between ($\lambda \sim 1$) should correspond to smoothing of discontinuities in instantaneous force pulses. This implies that motor activities are more correlated and continuous for the actin cytoskeleton probed through the cell membrane than intracellular motors re-

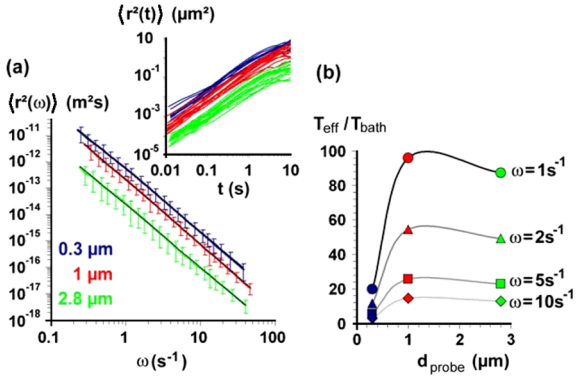

FIG. 4 (color online). (a) $\langle r^2(\omega)\rangle$ as a function of frequency for the three phagosome probes. Black lines correspond to the best fit with Eq. (3) $\langle r^2(\omega)\rangle = D(\omega/\omega_o)^{-(\beta+1)}$: $\beta = 1.38$, $\beta = 1.43$, and $\beta = 1.39$ and $D = 5.4 \times 10^{-13}$ m^2 s, $D = 2.2 \times 10^{-13}$ m^2 s, and $D = 2.4 \times 10^{-14}$ m^2 s for beads of 0.3, 1, and 2.8 μm diameters, respectively. Inset: MSD $\langle r^2(\Delta t)\rangle$ computed for each independent cell as $\langle r^2(\Delta t)\rangle = \langle [x(t+\Delta t) - x(t)]^2 + [y(t+\Delta t) - y(t)]^2\rangle$, where $(x, y)(t)$ is the bead position at time t, Δt is the time lag, and angle brackets denote averaging over t. (b) Effective temperature over the bath temperature as a function of the probe diameter d_{probe}. The set of equations (1)–(3) then gives the effective temperature T_{eff} for the nonequilibrium situation: $k_B T_{\text{eff}}(\omega) = \frac{3\pi a D G_o}{2\sin(\pi\alpha/2)}(\omega/\omega_o)^{\alpha-\beta}$, with $\omega_o = 1$ s^{-1}. The lines are visual guides.

sponsible for phagosome transport. Besides, thanks to independent measurements of intracellular stiffness and mean square displacement, we derive quantitatively the force fluctuation spectrum. As it follows power-law behavior, the Fourier transform $P_{FF}(\omega)$ is easily inverted, leading to the force correlation function:

$$\langle F(t)F(t+\tau)\rangle_t = F_o\left(\frac{\tau}{\tau_o}\right)^{\lambda-1}, \quad (6)$$

with τ_o set to 1 s and F_o equal to 0.4, 2.7, and 5.7 pN for 0.3-, 1-, and 2.8-μm beads, respectively. The force correlation increases slightly with time in the probed time range (0.01–1 s) with an exponent of about 0.2, a signature of collective behavior with reinforcement of the force with time, and an average value in the range of the stall force of a single kinesin motor, which is about 5 pN. If one keeps in mind the picture of molecular motors generating forces in discontinuous force pulses, these statistical mean values of the active forces are not unreasonable and support the vision of cooperative motors acting together for active transport of phagosome cargos [16].

The measured $P_{FF}(\omega)$ exhibit a strong mismatch with the prediction at thermal equilibrium [Eq. (3)], demonstrating that the fluctuation-dissipation theorem is no longer valid inside living cells. To quantify the deviation from the in-equilibrium situation, it has been proposed to replace the bath temperature T in Eqs. (2) and (3) by a frequency-dependent effective temperature T_{eff} [17]. $T_{\text{eff}}(\omega)$ then runs roughly as $\omega^{-0.8}$, for the accessible frequency range (0.1–10 Hz): The lower the frequency, the higher the effective temperature. Deviation from equilibrium is due to the action of phagosome driving motors, the activities of which should not interfere with high-frequency thermal modes. Figure 4(b) shows the ratio of the effective temperature to the bath temperature (37 °C) as a function of the probe diameter and at different frequencies. With 0.3-μm-diameter probes, we found an effective temperature that is 20 times the bath temperature at 1 s^{-1}. By contrast, the effective temperature is almost a hundredfold the bath temperature with 1- and 2.8-μm-diameter beads at 1 s^{-1}. The phagosomes of 0.3 μm diameter have fewer interactions with the networks, whereas phagosomes 1 and 2.8 μm in diameter are more likely to come across cytoskeleton filaments and undergo active transport.

In conclusion, using active magnetic bead rotational microrheology, it is demonstrated that the intracellular shear modulus has a power-law dynamics of exponent between 0.5–0.6: The inside of the cell has a more liquid-like behavior than the membrane and associated cytoskeleton. In addition, the absolute value of the shear modulus increases with the probe size, reflecting structural complexity. By combining this active intracellular microrheology with classical passive microrheology, this Letter exhibits a strong violation of the fluctuation-dissipation theorem inside the cells. This deviation from the in-equilibrium situation was estimated by measuring a frequency-dependent effective temperature different from the bath temperature or, alternatively, the power spectrum of active intracellular forces, both of which are directly coupled to the activity of biological motors.

The author acknowledges Jean-Claude Bacri, Damien Robert, Florence Gazeau, and François Gallet for fruitful discussions and Jacques Servais for technical help.

*claire.wilhelm@univ-paris-diderot.fr

[1] N. Desprat, A. Richert, J. Simeon, and A. Asnacios, Biophys. J. **88**, 2224 (2005).
[2] B. Fabry, G. N. Maksym, J. P. Butler, M. Glogauer, D. Navajas, and J. J. Fredberg, Phys. Rev. Lett. **87**, 148102 (2001).
[3] J. Alcaraz, L. Buscemi, M. Grabulosa, X. Trepat, B. Fabry, R. Farre, and D. Navajas, Biophys. J. **84**, 2071 (2003).
[4] M. Balland, N. Desprat, D. Icard, S. Féréol, A. Asnacios, J. Browaeys, S. Hénon, and F. Gallet, Phys. Rev. E **74**, 021911 (2006).
[5] W. Feneberg, M. Westphal, and E. Sackmann, Eur. Biophys. J. **30**, 284 (2001).
[6] S. Marion, N. Guillen, J.-C. Bacri, and C. Wilhelm, Eur. Biophys. J. **34**, 262 (2005).
[7] M. Yanai, J. P. Butler, T. Suzuki, H. Sasaki, and H. Higuchi, Am. J. Physiol. **287**, C603 (2004).
[8] S. Yamada, D. Wirtz, and S. C. Kuo, Biophys. J. **78**, 1736 (2000).
[9] Y. Tseng, T. P. Kole, and D. Wirtz, Biophys. J. **83**, 3162 (2002).
[10] A. Caspi, R. Granek, and M. Elbaum, Phys. Rev. Lett. **85**, 5655 (2000).
[11] D. Mizuno, C. Tardin, C. F. Schmidt, and F. C. Mackintosh, Science **315**, 370 (2007).
[12] P. Bursac, G. Lenormand, B. Fabry, M. Oliver, D. A. Weitz, V. Viasnoff, J. Butler, and J. J. Fredberg, Nat. Mater. **4**, 557 (2005); P. Bursac, B. Fabry, X. Trepat, G. Lenormand, J. P. Butler, N. Wang, J. J. Fredberg, and S. S. An, Biochem. Biophys. Res. Commun. **355**, 324 (2007).
[13] C. Wilhelm, J. Browaeys, A. Ponton, and J. C. Bacri, Phys. Rev. E **67**, 011504 (2003).
[14] C. Wilhelm, F. Gazeau, and J. C. Bacri, Phys. Rev. E **67**, 061908 (2003).
[15] A. W. C. Lau, B. D. Hoffmann, A. Davies, J. C. Crocker, and T. C. Lubensky, Phys. Rev. Lett. **91**, 198101 (2003).
[16] K. B. Zeldovich, J. F. Joanny, and J. Prost, Eur. Phys. J. E **17**, 155 (2005); S. Klumpp and R. Lipowsky, Proc. Natl. Acad. Sci. U.S.A. **102**, 17 284 (2005).
[17] N. Pottier, Physica (Amsterdam) **345A**, 472 (2005); B. Abou and F. Gallet, Phys. Rev. Lett. **93**, 160603 (2004); S. Jabbari-Farouji *et al.*, Phys. Rev. Lett. **98**, 108302 (2007).
[18] See EPAPS Document No. E-PRLTAO-101-068827 for two videos showing the oscillations of chains of magnetic phagosomes at 0.2 and 2 Hz frequencies. For more information on EPAPS, see http://www.aip.org/pubservs/epaps.html.